

Bionic Soft Fingers with Hybrid Variable Stiffness Mechanisms for Multimode Grasping

Xiangbo Wang^{1,2}, Tianran Zhang³, Hongze Yu⁴, Zhenwei Wen³, Lide Fang¹, Huaping Liu⁵,
Fuchun Sun⁵, Lixue Tang⁶ and Bin Fang^{2*}

Abstract—This paper presents a novel Bionic Soft Finger (BSF) that aims to overcome the limitations of conventional rigid manipulators in terms of adaptability and safety, as well as the challenges faced by soft hands regarding carrying capacity and stability. The BSF design uses a hybrid variable stiffness mechanism combining memory alloy actuators with particle jamming to achieve the desired bending angle and actuator stiffness. Our innovative approach utilizes a bionic finger design that incorporates a memory alloy skeleton and a water-cooled recirculation system, leading to a substantial reduction in the time required for each operation. Through the integration of particle jamming, we have enhanced the overall stiffness and performance of the manipulator, enabling load capacities of up to 3N per finger and more than twice the stiffness of a normal condition. Additionally, our design enables multimode grasping and incorporates a liquid metal strain sensor (METT) for real-time monitoring of finger bending angles. Comparative analyses demonstrate that our design exhibits superior stiffness and enables five-mode grasping in comparison to pneumatic actuators. We believe that bionic soft fingers present a promising solution for enhancing adaptability, safety, and performance in human-robot interaction applications.

I. INTRODUCTION

Traditional mechanical grippers are inspired by primates and their biological end-effectors. However, their high rigidity limits adaptability and safety in human-robot interaction [1], [2]. Soft grippers have emerged to overcome these inherent flaws and shortcomings [3], [4].

They possess distinctive characteristics that differentiate them from rigid grippers. Featuring soft surfaces, malleable materials, and elastic actuators, soft grippers display a natural gentleness when manipulating objects [5]. However, the incorporation of soft elastic materials in their construction often results in reduced load-carrying capacity and stiffness,

thereby restricting their ability to handle heavier objects and introducing instability during grasping.

To counter these limitations, various techniques have been proposed to enhance the stiffness of soft grippers. Incorporating low-melting-point alloys into soft actuators grants the flexibility to manipulate mechanical degrees of freedom and stiffness [6]. Furthermore, the combination of variable-stiffness endoskeletons with pneumatic actuators enables the bending of a single actuator at multiple points [7]. However, the integration of additional actuator primitives remains necessary. Pneumatic actuators moderately enhance stiffness and expand the contact area with objects through adjustments in shape, wall thickness, size, and the number of chambers [8], [9]. Yet, the improvements in rigidity achieved through these modifications are often limited. The complexity of constructing intricate soft structures with precise material dimensions tends to increase manufacturing costs. Tendon actuation requires intricate internal structures, and the wear and tear of internal motors and tendons significantly impact performance [10], [11]. The shape memory effect allows memory materials to exhibit various changes in attitude and stiffness by adjusting the temperature appropriately [12]. Shape memory alloy wires (SMAs), which are frequently utilized as soft actuators, often face limitations regarding heat accumulation [13] and low clamping force [14].

Researchers have recently explored the combination of actuation methods with obstruction to enhance the overall stiffness of the actuator. Examples include tendon-driven gripper jaws combined with layer obstruction [15], [16] and tendon-driven grippers combined with particle obstruction [17]. These approaches not only increase stiffness but also provide additional functionalities to the soft gripper.

In this paper, we introduce a novel design of the Bionic Soft Finger (BSF) that incorporates a memory alloy actuator and particle jamming mechanism. This integration ensures the preservation of the required bending angle and actuator stiffness, resulting in a substantial enhancement in efficiency. Our innovative design overcomes the limitations of previous approaches by:

- Implementing a bionic finger design that employs a memory alloy as the backbone, combined with a water-cooled structure serving as the circulation system.
- Utilizing a hybrid mechanism that combines particle jamming and SMA enhances the overall stiffness and performance.
- Introducing multimode grasping enables the manipulator to adapt to various tasks, where real-time monitoring

*This work was supported by the National Natural Science Foundation of China under Grant 62173197, CIE-Tencent Robotics X Rhino-Bird Focused Research Program under Grant 2022-01

¹College of Quality and Technical Supervision, Hebei University, Baoding 071002, China (email:15369902997@163.com; fanglide@hbu.edu.cn)

²School of Artificial Intelligence, Beijing University of Posts and Telecommunications, Beijing 100876, China

³School of Mechanical Engineering & Automation, Beihang University, Beijing, Haidian 100191, China

⁴International School, Beijing University of Posts and Telecommunications, Beijing 100876, China

⁵Institute for Artificial Intelligence, State Key Lab of Intelligent Technology and Systems, Department of Computer Science and Technology, Beijing National Research Center for Information Science and Technology, Tsinghua University, Beijing 100084, China

⁶School of Biomedical Engineering Beijing Key Laboratory of Fundamental Research on Biomechanics in Clinical Application Capital Medical University No.10 Xitoutiao, You An Men Wai, Beijing 100069, China

*Corresponding author: Bin Fang.fangbin120@bupt.edu.cn

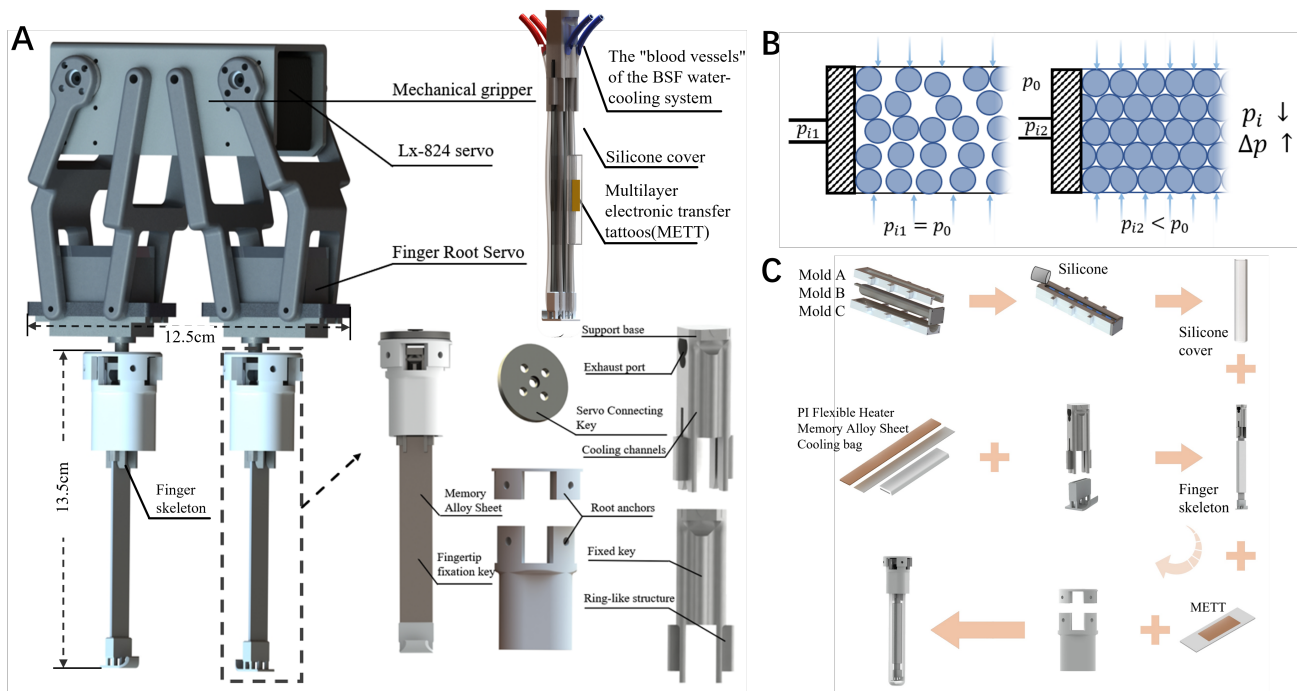


Fig. 1. CAD model of Bionic soft finger (BSF) (A): Holistic structure of Mechanical gripper and BSF. To achieve optimal stiffness, the finger bones are constructed using a combination of aluminum alloy and nickel-titanium alloy (memory alloy), while the remaining sections of the fingers are made from resin-plastic materials. (B): Principle of particle jamming. (C): Fabrication process diagram of bionic soft fingers. Cooling bags are simplified by a combination of silicone tubes. METT: Has metal-grade electrical conductivity (4-6 orders of magnitude higher than hydrogel), hydrogel-grade stretchability (>900%) and self-adhesion.

of finger flexion angles using a liquid metal strain sensor (METT) [18]–[20].

II. DESIGN AND STRUCTURE

A. Structure

Figure 1A illustrates the composition of the BSF, which consists of a mechanical gripper and a soft finger. Equipped with two Lx-824 servos and a transmission mechanism, the mechanical gripper allows for a stroke range of 0 to 13 cm.

The overall structure of the soft finger includes a finger root servo, root anchors, and a finger skeleton. Initially, a memory alloy sheet is attached to the fingertip fixation key. It is then inserted into the ring-like structure of the fixed key and embedded at the center to form the finger skeleton. To ensure stability, four screws firmly secure the root anchors to the support platform.

Through the utilization of a servo connection key, the soft finger establishes a vital connection with the root servo, facilitating and enabling the crucial capability of circumferential rotation. This connection mechanism empowers the soft finger to rotate circularly, significantly expanding its range of motion and enhancing its dexterity. By combining the mechanical jaws with rotational characteristics, the soft finger becomes flexible and versatile. Additionally, it enables various hand operations and precise control in complex environments.

Inspired by the human hand, the design of the bionic finger combines a rigid finger skeleton with a silicone shell. It

incorporates various features, including SMA actuation, variable stiffness, and active cooling. The SMA actuation system consists of PI heating pads and memory alloys, supplemented by cooling pockets to dissipate heat accumulation.

To fabricate the finger, silicone 0050 is cast into a 3D-printed mold for release. Pressure sensors are attached to the inner wall of the silicone sleeve, enabling self-sensing of bending angles as depicted in Figure 1C. During the assembly process, the silicone shell and finger skeleton create a spacious internal cavity. The key to stiffness adjustment lies within this cavity, which contains particles. By connecting a vacuum pump to the fixture's exhaust port using a pipe, the air between the particles can be removed, altering the finger's stiffness.

Compared to [21], [22], this design is more simplified and compact, measuring only 13 cm in total length. It ensures both finger flexibility and grasping functionality. By integrating a rigid skeleton, a soft shell, an SMA actuator, and a variable stiffness mechanism, the bionic finger successfully achieves a human-like grasping function. This innovative and compact design showcases its uniqueness.

B. Variable stiffness principle

Shape memory alloys (SMAs) are commonly utilized as actuators in soft hands, providing a considerable degree of bending. On account of the shape memory effect, SMAs can adapt their shape based on temperature conditions. The active deformation forces generated during the heating and bending of SMAs determine the bending angle and speed of the fin-

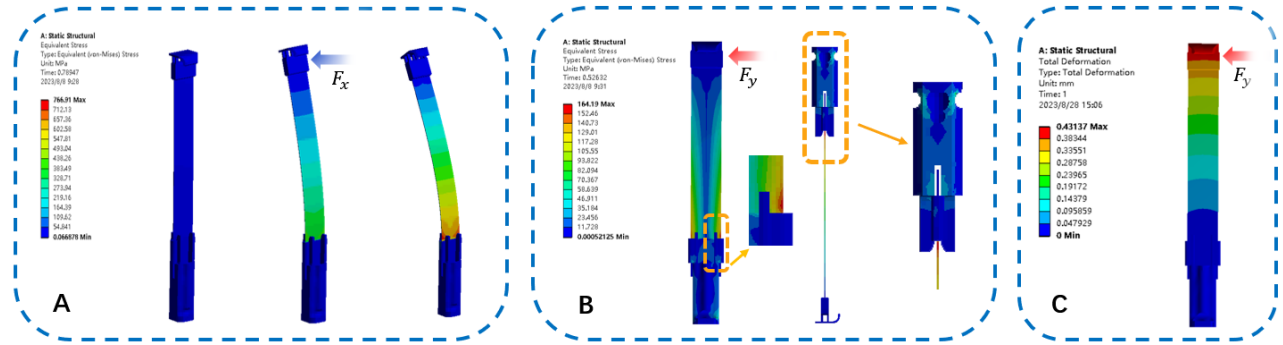


Fig. 2. FEM simulation of skeleton stresses in BSFs.(A)and(B):Stress distribution in the finger skeleton.(C):Displacement vector of finger skeleton.

gers. The active deformation force resulting from the phase transition of SMAs enables precise control over the bending angle and speed of the robotic finger. However, in [23] and [24], while the memory alloy wire demonstrates favorable bending performance, there is still a need for enhancement in its load capacity. There exists an inverse relationship between the load-bearing capacity of the memory alloy sheet and its degree of bending, making it impossible to achieve simultaneously.

In this paper, we propose a combination of two variable stiffness methods. By optimizing the particle parameters, as described in Section II.C, their impact on soft finger performance can be minimized. As illustrated in Figure 1B, the application of a negative pressure environment triggers the rearrangement of particles within the cavity. These particles bind firmly together, forming a rigid structure that effectively resists deformation. This integration of programmable actuation and variable particle stiffness mechanisms allows for the realization of advanced gripping and manipulation capabilities.

C. Selection of filling materials

The stiffness of the finger is directly influenced by the size and roughness of the filling material under negative pressure conditions. Four granular materials were tested in this study: ground glass, millet, rice, and adzuki bean. The results indicate that the resistance generated by using millet as a filler is 1.35 times that of rice and 4.65 times that of adzuki beans. However, the use of ground glass as a filler did not significantly enhance the stiffness. That is because of the continued relative sliding behavior under negative pressure conditions. Figure 3 demonstrates how particle properties impact the stiffness.

Particle size directly influences the finger's bending range, with larger particles imposing greater restrictions on the bending radius. During finger bending, the particles undergo compression and rearrangement, leading to a progressive increase in friction. At the maximum bending position, the accumulated friction between the particles opposes the bending force of the actuator.

As shown in Fig. 1B, the particles inside the chamber are freely arranged with significant gaps between them under

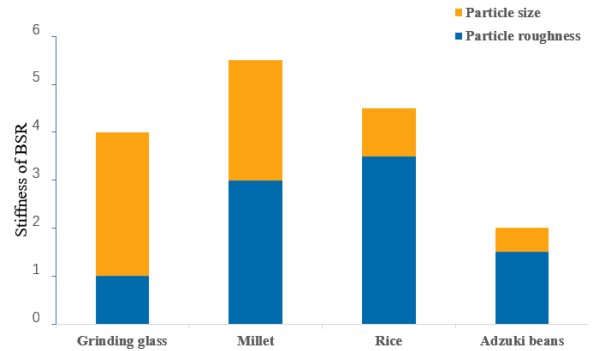


Fig. 3. Influence of filler material properties on finger stiffness

normal pressure. External pressure induces relative sliding and reassembly of the particles. Under negative pressure, these gaps decrease, causing the particles to align tightly and preventing structural deformation due to friction. However, smaller and smoother particles, such as the abrasive glass used in the experiment, can still experience relative sliding under negative pressure.

III. FINITE ELEMENT SIMULATION

To investigate the robustness and structural effectiveness of the BSF, we employed finite element analysis (FEA) tools to delve into the inherent mechanical properties of the finger assembly.

When a human hand grips an object, the exerted forces can be classified into horizontal forces (F_x) and vertical forces (F_y). The vertical force primarily carries the weight of the object, while the horizontal force ensures the object's stability. The soft hand is extremely similar to the human hand in its gripping pattern. Therefore, it is required to have excellent bending resistance to support the weight of the object vertically, and the ability to provide a significant level of friction horizontally.

To quantify the structural effectiveness of the finger skeleton, we conducted two specialized experiments. As depicted in Figure 2(A), the application of F_x induces bending deformation in the memory alloy sheet, with stress concentrations primarily occurring near the ring structure.

Excessive application of F_y leads to irreversible damage, such as tearing, of the memory alloy sheet. In the simulation experiment, a force of 31N was applied, resulting in significant stress accumulation on the side of the memory alloy sheet and the fixed key. Consequently, we observed a slight displacement of the fingertip, approximately 0.5mm, as illustrated in Figures 2(B) and (C). These findings can fulfill our needs.

The unique characteristics of the skeleton structure result in significantly smaller displacement in the vertical (Y) direction compared to the horizontal (X) direction when subjected to the same magnitude of force. The flat and sturdy support on the sides of the fingers provides favorable conditions. The method of pinching with a single finger takes advantage of this, allowing for a larger contact area and achieving a more stable grip, as depicted in the first panel of Figure 6.

The experimental results highlight that the forces borne by the finger predominantly act upon the root of the ring structure and the memory alloy sheet. Fortunately, the ring structure effectively provides support and protection for the memory alloy sheet, thereby confirming the efficacy of our design.

IV. MULTIMODE GRASPING CONTROL STRATEGY

The bending characteristics of SMAs are primarily influenced by temperature variations. A systematic approach was adopted to facilitate controlled finger bending and recovery, thereby ensuring effective gripping of the gripper.

Initially, the control board sends control commands to select the appropriate gripping mode. The transitions between each state occur at intervals of approximately 0.5 seconds. During the gripping process, a PI heating pad is utilized to apply the required heat to the finger, inducing the shape transformation of the SMA and enabling the finger to bend at an appropriate angle for the gripping operation. Lastly, a water-cooled structure is employed to establish a low-temperature environment that facilitates the recovery and return of the finger to its initial position.

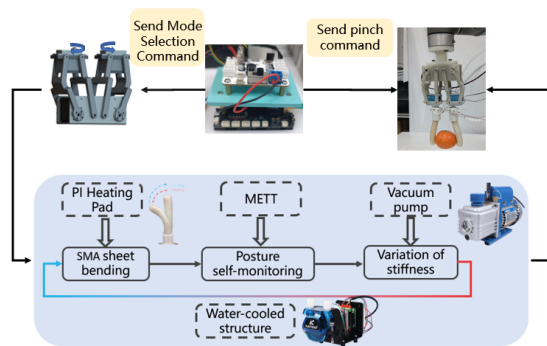


Fig. 4. Multi-grasping Control Strategy

To precisely monitor finger posture, the METT is utilized to observe the finger's bending posture, accurately measure

its bending angle, and provide real-time feedback on deformations. Figure 5 demonstrates the response of the METT to finger flexion angles.

To ensure proper implementation of the clamping operation, a vacuum pump is employed to establish a controlled vacuum environment that effectively alters the finger's stiffness. Figure 4 depicts the process involving heating using a PI heating pad, cryogenic cycling through a water-cooled structure, finger posture monitoring with the METT, and stiffness adjustment with the vacuum pump. This systematic approach leads to a successful finger flexion and recovery process, guaranteeing stable positioning of the finger in the desired position. This process establishes a dependable foundation for precise finger control and movement within the system.

V. EXPERIMENTS

A. Cooling effect of liquid circulation

This study presents a bionic soft actuator with a novel water-cooled structure designed to enhance heat dissipation efficiency. Inspired by the human blood circulation system, the structure aims to mimic its functionality. The water-cooled structure consists of a KCM-B163-ODMA micro-circulation pump and cooling pockets, representing the heart and blood vessels, respectively. These components are responsible for efficient heat transfer and dissipation.

TABLE I
COMPARISON BETWEEN RTC AND W-C

Methods	1	2	3	4	5	6	7
RTC	94	168	235	268	311	308	304
	59	91	124	154	224	304	311
	61	98	145	201	242	301	307
W-C	34	26	27	29	28	30	26
	24	22	26	29	26	27	29
	24	31	29	31	28	32	31

RTC: Room temperature condition.
W-C: Water-cooling condition.

In contrast to pressure-dependent diaphragm pumps, the circulation pump operates by cycling a flexible hose segment

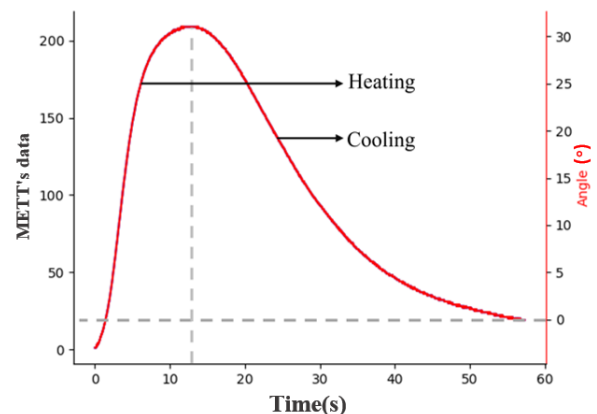


Fig. 5. BSF Single Cooling Time and Bending Angle Reflected by METT.



Fig. 6. Multi-modal capture of BSF. The BSF’s multi-mode grasping capabilities are achieved through mode switching, facilitated by the rotation of the root servo and the bending of each finger.

between two wheels, enabling compression and decompression. This mechanism ensures a continuous flow of fluid within the tubing, enhancing pressure resistance.

In a healthy human body, approximately 5 kilocalories of heat are emitted per minute, and the circulatory system plays a vital role in the heat dissipation process. Similarly, the Bionic Actuator circulates accumulated heat through the fluid within the water-cooled structure, resulting in an impressive 1071% increase in overall heat dissipation efficiency compared to conventional methods.

The integration of the BSF significantly improves the overall operational efficiency of the system, demonstrating a notable enhancement of over 110% compared to the results reported in [13].

The experimental results underscore the effectiveness of the novel water-cooled structure in improving the thermal efficiency of the bionic soft actuator. These findings have important implications for the development of more efficient and reliable soft robotic systems in various applications.

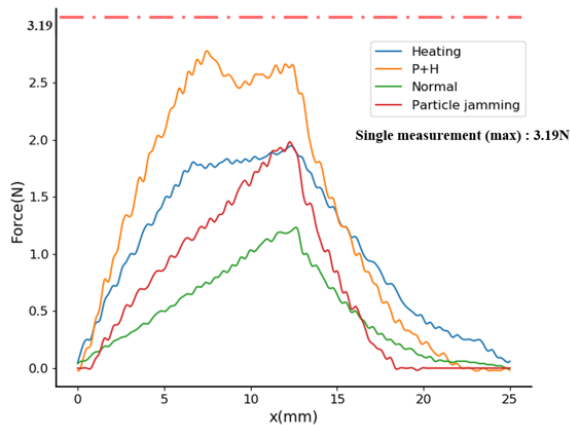


Fig. 7. Experimental results on stiffness forces of soft fingers applying different types of variable stiffness methods. Maximum value of single measurement: 3.19N

Experimental results indicate that the conventional actuator structure fails to dissipate internal heat adequately after multiple heating cycles, leading to progressively longer recovery times. However, the integration of the water-cooled

structure allows timely heat dissipation, significantly enhancing recovery efficiency. This efficiency remains stable, with a consistent 5% variation rate.

B. Variable stiffness experiment

To evaluate the variable stiffness performance, we built a force measurement platform comprising a force gauge mounted on a three-axis motion stage with a measurement accuracy of 0.2 N. The platform also included a fixture, a finger-holding fixture, and a vacuum pump for creating a vacuum environment. We performed variable stiffness performance tests in four scenarios: normal state, heating state, particle-jamming state, and simultaneous heating and particle-jamming state.

We maintained a consistent moving distance of 25 mm for each test case to ensure consistency. The memory alloy sheet exhibited substantial improvements in variable stiffness performance compared to the normal condition, achieving performance enhancements of 1.59 times (heating condition), 1.62 times (particle-jamming condition), and 2.27 times (heating and particle-jamming condition). These findings highlight the adaptability and performance of memory alloys across diverse conditions.

Measurements taken on the force platform indicated a maximum load capacity of 2.77 N for the BSF. It is worth noting that when the BSF is pressed in a straight manner, there is a slight slippage relative to the indenter of the force gauge, which leads to the sudden downward shift observed in the curve shown in Figure 7.

In a separate measurement, the maximum load capacity of an individual finger was found to be 3.19 N, surpassing the load capacity of the pneumatic gripper. This hybrid variable stiffness mechanism greatly enhances the load-carrying capacity of the BSF.

C. Grasping experiment

We conducted a series of experiments to examine the capability of BSF to imitate human grasping movements. The four primary human grasping movements are enveloping, pinching, hooking (hanging), and embedding. Examples comprise grasping an orange on a table, pinching a thin sheet-like object with the fingers, and hanging a shopping bag.

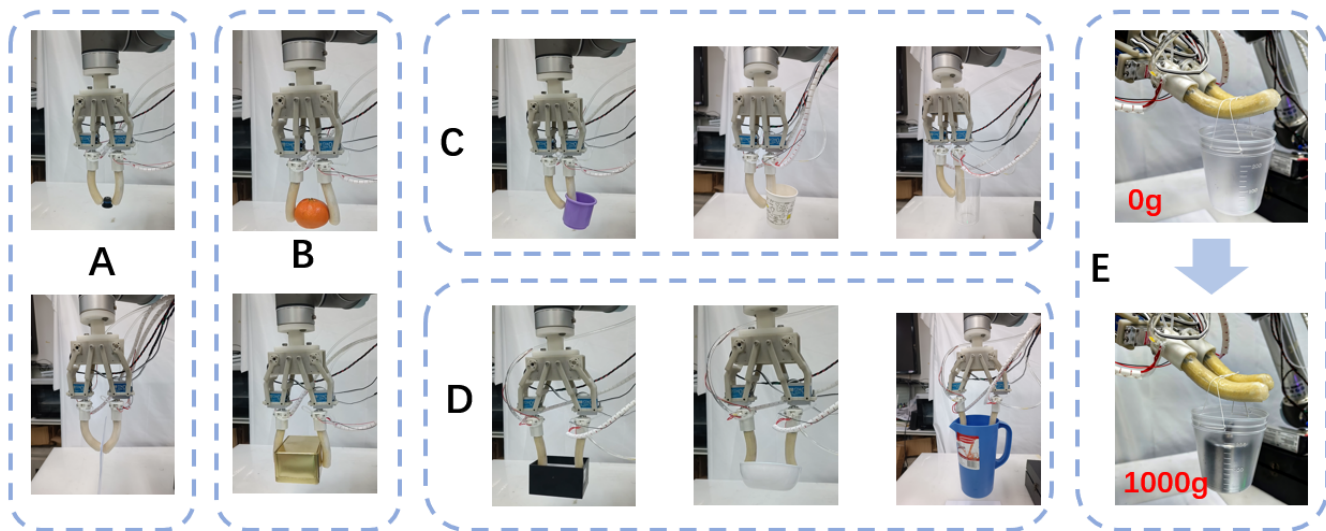


Fig. 8. Multi-mode grasping experiment. (A): pinching(The pinch grip is better suited for grasping smaller objects, as this grip configuration allows for a greater concentration of gripping force within a smaller area compared to a parallel grasp.) (B): enveloping (C): single finger pinching (D): expansion grasping (E): Experiments were conducted on the BSF with adjusted stiffness to test its load-bearing capacity with different weights.

Figure 8 demonstrates the diverse grasping modes supported by the BSF. This illustration reveals that soft grippers extend beyond envelopes and pinches to include expansion grasping modes.

The silicone sleeve functions as the "skin" of the BSF, allowing the gripper to securely grasp objects without causing any damage. Furthermore, a hybrid variable stiffness mechanism improves the load-carrying capacity of the manipulator. To assess the soft gripper's adaptability to various objects, a collection of household objects with different stiffnesses, weights, and shapes was chosen. The soft gripper employs various grasping modes for these objects.

The memory alloy's active bending properties provide the BSF with excellent wrapping capabilities. The BSF securely grasps the orange, as depicted in Figure 8. The hybrid variable stiffness mechanism enhances the stability of the gripper jaws when gripping thin, light, and small objects. The single-finger pinch grip position is advantageous for cup gripping, this position offers a larger contact area compared to point-to-point contact. Embedding the fingers within the cup increases the contact area, improving the grip and interaction between the gripper and the cup's inner surface.

Nevertheless, the smooth surfaces and objects that exceed the gripper transfer mechanism's range of motion, such as bowls and large-caliber objects, can pose challenges for gripping. In contrast to previous methods, we achieve the grasping of such objects by modifying the finger posture instead of actively adjusting the gripper's effective range of motion. The finger posture is adjusted by rotating the base servo, as illustrated in Figure 8(D). Expansion grasping provides internal support to the object, enhancing its reliability in comparison to gripping on smooth surfaces.

We conducted a series of hanging tests to evaluate the finger's load-bearing capacity, with a maximum weight of

1000g. As depicted in Figure 8(E), the curvature of the finger gradually decreased with increasing weight. The finger progressively bent downwards, following the simulation results, and the weight was supported by the finger's root connection.

The experimental results underscore the effectiveness of the BSF design, demonstrating its capability to withstand significant loads. The increased load-carrying capacity of the BSF creates opportunities for its utilization in diverse fields, such as logistics, industrial automation, and human-robot interaction.

VI. CONCLUSION AND FUTURE WORK

Our study on Bionic Soft Fingers (BSF) proposes the utilization of diverse components to replicate the intricate structure of a human hand. The design comprises a memory alloy skeleton, particle-jamming muscles, silicone sleeves for the skin, and water-cooling systems. To enhance efficiency, we have implemented a water-cooling system that reduces the cooling time for each operation to a mere 30 seconds.

The hybrid variable stiffness mechanism, combining memory alloy and particle jamming, enables our BSF to surpass traditional pneumatic grippers, achieving a load-bearing capacity of 3.19 N. Furthermore, the rotation of the root servo enhances the manipulation capabilities of the soft finger, giving the BSF a competitive advantage in practical applications.

In our future work, we will enhance the functionality of the liquid metal strain sensor (METT) and integrate its signals with the heating system as a vital control parameter. This integration will enable the soft hand to actively adapt to the surface curvature of objects.

REFERENCES

- [1] M. Pozzi, S. Marullo, G. Salvietti, J. Bimbo, M. Malvezzi, and D. Prattichizzo, "Hand closure model for planning top grasps with

- soft robotic hands,” *The International Journal of Robotics Research*, vol. 39, no. 14, pp. 1706–1723, 2020.
- [2] S. Zhang, J. Shan, B. Fang, F. Sun, and H. Liu, “Vision-based tactile perception for soft robotic hand,” in *2019 IEEE International Conference on Robotics and Biomimetics (ROBIO)*, pp. 621–628, IEEE, 2019.
- [3] J. Shintake, V. Cacucciolo, D. Floreano, and H. Shea, “Soft robotic grippers,” *Advanced Materials*, p. 1707035, Jul 2018.
- [4] R. Deimel and O. Brock, “A novel type of compliant and underactuated robotic hand for dexterous grasping,” *The International Journal of Robotics Research*, vol. 35, no. 1-3, pp. 161–185, 2016.
- [5] C. Della Santina, M. G. Catalano, A. Bicchi, M. Ang, O. Khatib, and B. Siciliano, “Soft robots,” *Encyclopedia of Robotics*, vol. 489, 2020.
- [6] Y. Hao, T. Wang, and L. Wen, “A programmable mechanical freedom and variable stiffness soft actuator with low melting point alloy,” in *International Conference on Intelligent Robotics and Applications*, 2017.
- [7] S. Yoshida, Y. Morimoto, L. Zheng, H. Onoe, and S. Takeuchi, “Multipoint bending and shape retention of a pneumatic bending actuator by a variable stiffness endoskeleton,” *Soft robotics*, vol. 5, no. 6, pp. 718–725, 2018.
- [8] S. Zhao, D. Li, and J. Xiang, “Design and application of pneunets bending actuator,” *Aircraft Engineering and Aerospace Technology*, vol. 92, no. 10, pp. 1539–1546, 2020.
- [9] S. Zhang, J. Shan, B. Fang, and F. Sun, “Soft robotic finger embedded with visual sensor for bending perception,” *Robotica*, vol. 39, no. 3, pp. 378–390, 2021.
- [10] M. Dragusanu, D. Troisi, D. Prattichizzo, and M. Malvezzi, “Compliant finger joint with controlled variable stiffness based on twisted strings actuation,”
- [11] J. Yan, H. Zheng, F. Sun, H. Liu, Y. Song, and B. Fang, “C-shaped bidirectional stiffness joint design for anthropomorphic hand,” *IEEE Robotics and Automation Letters*, vol. 7, no. 4, pp. 12371–12378, 2022.
- [12] J. Mohd Jani, M. Leary, A. Subic, and M. A. Gibson, “A review of shape memory alloy research, applications and opportunities,” *Materials & Design (1980-2015)*, p. 1078–1113, Apr 2014.
- [13] P. Do, N. Le, V. Luong, H.-H. Kim, H.-M. Park, and Y.-J. Kim, “Tendon-driven gripper with variable stiffness joint and water-cooled sma springs,”
- [14] W. Wang and S.-H. Ahn, “Shape memory alloy-based soft gripper with variable stiffness for compliant and effective grasping,” *Soft Robotics*, vol. 4, p. 379–389, Dec 2017.
- [15] B. Fang, F. Sun, L. Wu, F. Liu, X. Wang, H. Huang, W. Huang, H. Liu, and L. Wen, “Multimode grasping soft gripper achieved by layer jamming structure and tendon-driven mechanism,” *Soft Robotics*, vol. 9, no. 2, pp. 233–249, 2022.
- [16] F. Liu, F. Sun, B. Fang, X. Li, S. Sun, and H. Liu, “Hybrid robotic grasping with a soft multimodal gripper and a deep multistage learning scheme,” *IEEE Transactions on Robotics*, vol. 39, no. 3, pp. 2379–2399, 2023.
- [17] M. Dragusanu, G. M. Achilli, M. C. Valigi, D. Prattichizzo, M. Malvezzi, and G. Salvietti, “The wavejoints: A novel methodology to design soft-rigid grippers made by monolithic 3d printed fingers with adjustable joint stiffness,” in *2022 International Conference on Robotics and Automation (ICRA)*, pp. 6173–6179, IEEE, 2022.
- [18] L. Tang, J. Shang, and X. Jiang, “Multilayered electronic transfer tattoo that can enable the crease amplification effect,” *Science Advances*, Jan 2021.
- [19] L. Tang, S. Yang, K. Zhang, and X. Jiang, “Skin electronics from bio-compatible in situ welding enabled by intrinsically sticky conductors,” *Advanced Science*, Aug 2022.
- [20] L. Yuyao, G. Yang, S. Wang, Y. Zhang, Y. Jian, L. He, T. Yu, H. Luo, D. Kong, Y. Xianyu, B. Liang, T. Liu, X. Quyang, J. Yu, X. Hu, H. Yang, Z. Gu, and W. . X. K. Huang, “Stretchable graphene–hydrogel interfaces for wearable and implantable bioelectronics,” *Nat Electron*.
- [21] P. Do, N. Le, V. Luong, H.-H. Kim, H.-M. Park, and Y.-J. Kim, “Tendon-driven gripper with variable stiffness joint and water-cooled sma springs,”
- [22] Y. Yang, Y. Zhang, Z. Kan, J. Zeng, and M. Y. Wang, “Hybrid jamming for bioinspired soft robotic fingers,” *Soft Robotics*, vol. 7, p. 292–308, Jun 2020.
- [23] W. Wang and S.-H. Ahn, “Shape memory alloy-based soft gripper with variable stiffness for compliant and effective grasping,” *Soft Robotics*, p. 379–389, Dec 2017.
- [24] Y. Haibin, K. Cheng, L. Junfeng, and Y. Guilin, “Modeling of grasping force for a soft robotic gripper with variable stiffness,” *Mechanism and Machine Theory*, p. 254–274, Oct 2018.